Biochemical and Biophysical Research Communications 723 (2024) 150153

Contents lists available at ScienceDirect

Biochemical and Biophysical Research Communications

journal homepage: www.elsevier.com/locate/ybbrc

Visualization of Reissner's membrane in the mouse inner ear using highly sensitive magnetic resonance imaging analysis

Shotaro Harada [a,b], Yoshihisa Koyama [a,c,d,e,*], Yoshichika Yoshioka [f,g,h], Hidenori Inohara [b], Shoichi Shimada [a,c,d]

[a] Department of Neuroscience and Cell Biology, Osaka University Graduate School of Medicine, Osaka 565-0871, Japan
[b] Department of Otorhinolaryngology-Head and Neck Surgery, Osaka University Graduate School of Medicine, Suita, Osaka 565-0871, Japan
[c] Addiction Research Unit, Osaka Psychiatric Research Center, Osaka Psychiatric Medical Center, Osaka, 541-8567, Japan
[d] Global Center for Medical Engineering and Informatics, Osaka University, Suita, 565-0871, Japan
[e] Integrated Frontier Research for Medical Science Division, Institute for Open and Transdisciplinary Research Initiatives (OTRI), Osaka University, Suita 565-0871, Japan
[f] Graduate School of Frontier Biosciences, Osaka University, Osaka 565-0871, Japan
[g] Center for Information and Neural Networks, National Institute of Information and Communications Technology (NICT) and Osaka University, Osaka 565-0871, Japan
[h] Institute for Open and Transdisciplinary Research Initiatives, Osaka University, Osaka 565-0871, Japan

ARTICLE INFO

Keywords:
Reissner's membrane
Magnetic resonance imaging
inner ear
ex vivo MRI
In vivo MRI

ABSTRACT

Although research on hearing loss, including the identification of causative genes, has become increasingly active, the pathogenic mechanism of hearing loss remains unclear. One of the reasons for this is that the structure of the inner ear of mice, which is commonly used as a genetically modified animal model, is too small and complex, making it difficult to accurately capture abnormalities and dynamic changes *in vivo*. Especially, Reissner's membrane is a very important structure that separates the perilymph and endolymph of the inner ear. This malformation or damage induces abnormalities in hearing and balance. Until now, imaging analyses, such as magnetic resonance imaging (MRI) and computed tomography, are performed to investigate the inner ear structure *in vivo*; however, it has been difficult to analyze the small inner ear structure of mice owing to resolution. Therefore, there is an urgent need to develop an image analysis method that can accurately capture the structure of the inner ear of mice including Reissner's membrane, both dynamically and statically.

This study aimed to investigate whether it is possible to accurately capture the structure (e.g., Reissner's membrane) and abnormalities of the inner ear of mice using an 11.7 T MRI. By combining two types of MRI methods, *in vivo* and *ex vivo*, we succeeded for the first time in capturing the fine structure of the normal mouse inner ear, such as the Reissner's membrane, and inflammatory lesions of otitis media mouse models in detail and accurately. In the future, we believe that understanding the state of Reissner's membrane during living conditions will greatly contribute to the development of research on inner ear issues, such as hearing loss.

1. Introduction

Recent advances in medical genetics have led to the elucidation of the genes that cause hearing loss [1,2]. Improvements in genetic recombination technology [3] have made it possible to prepare mouse models, such as transgenic and knockout mice; moreover, research to elucidate the causes of hearing loss is increasingly active. However, the mechanism by which the causative gene causes hearing loss remains unknown. One of the reasons for this is that the inner ear structure is too small and complex, making it impossible to identify the abnormal area in detail, and dynamic changes in the living organisms. Although imaging techniques such as magnetic resonance imaging (MRI) [4] and computed tomography [5] are used to capture the inner ear structure *in vivo*, it has been difficult to accurately analyze the structure of the small mouse inner ear because of resolution limitations. Therefore, there is a strong desire among inner ear researchers for a high-resolution image analysis method.

Reissner's membrane, a two-layered membrane located between the scala vestibuli and scala media in the inner ear, is a very important

* Corresponding author. Department of Neuroscience and Cell Biology, Osaka University Graduate School of Medicine, Osaka, 565-0871, Japan.
E-mail addresses: koyama@anat2.med.osaka-u.ac.jp (Y. Koyama), yoshioka@fbs.osaka-u.ac.jp (Y. Yoshioka), hinohara@ent.med.osaka-u.ac.jp (H. Inohara), shimada@anat1.med.osaka-u.ac.jp (S. Shimada).

https://doi.org/10.1016/j.bbrc.2024.150153
Received 10 May 2024; Accepted 20 May 2024
Available online 27 May 2024

Abbreviations

MRI	magnetic resonance imaging
LPS	lipopolysaccharide
3D	Three Dimension
PBS	phosphate-buffered saline
HE	hematoxylin and eosin

structure that separates the perilymph and endolymph. Reissner's membrane is greatly involved in endolymph homeostasis [6]. Therefore, stretching and cell density changes of Reissner's membrane cause endolymph hydrops [7]. Since endolymphatic hydrops cause hearing loss and vertigo, accurate understanding of *in vivo* condition of Reissner's membrane is extremely important in research in the field of otorhinolaryngology.

In this study, we investigated an effective i*n vivo/ex vivo* MRI method for inner ear analysis to identify Reissner's membrane using 11.7 T MRI.

2. Materials and methods

2.1. Animals and otitis media mouse models

Ten male C57B6/J mice, 6–8 weeks old, weighing 19–24 g (average 22.7 g; Japan SLC Co., Ltd., Shizuoka, Japan) were used in all experiments. Mice were kept in an environment with temperature, 23–25 °C, and humidity, 50 %). To induce inflammation in the middle ear, the tympanic membrane was penetrated from the left external auditory canal using a 27G needle, and 100 μl of saline containing 10 mg/ml lipopolysaccharide (LPS; Merck KGaA, Darmstadt, Germany) was injected into the left tympanic cavity; this was performed under anesthesia using a combination anesthetic (0.3 mg/kg medetomidine, 4.0 mg/kg midazolam, and 5.0 mg/kg butorphanol). The mouse was laid down with its left ear facing upward, and the LPS solution was kept in the tympanic cavity for 12 h until the mouse woke up from the anesthesia. Saline was administered to the right ear, which served as the contralateral control.

This study was conducted in strict accordance with the recommendations of the National Institutes of Health Guide for the Care and Use of Laboratory Animals. The study protocol was approved by the Committee of Animal Experiments of the Osaka University (approval numbers: 21-086-0, 27-043-000). This study was conducted according to the ARRIVE guidelines, minimizing the number of mice and their suffering as much as possible. If food or water was unavailable, food was placed on the bedding, and agar jelly was used as a supplement. In addition, if experimental mice exhibited abnormalities or hypothetical humane endpoints (e.g., difficulty feeding, drinking, or breathing, self-harm, rapid weight loss of 20 % or more over several days), animals were immediately euthanized by intraperitoneal administration of pentobarbital (200 mg/kg).

2.2. MRI analysis

In vivo and *ex vivo* MRI data were acquired using an 11.7 T scanner with ParaVision 6 (Bruker BioSpin, Ettlingen, Germany).

2.3. In vivo MRI

2.3.1. Mouse preparations

Gd MRI contrast agent (Gadoteridol, Eisai Co., Ltd., Tokyo, Japan) was injected intraperitoneally (100 μL/20 g body weight) to discriminate scala media from scala vestibuli and scala tympani by MRI [8]. MRI was performed 50–60 min after Gd injection. Anesthesia was initially induced with 2.0 % isoflurane and maintained with 1.6 % isoflurane during MRI. The body temperature of the mice was maintained at 37 °C with circulating warm water.

2.3.2. MRI

T_1 weighted sagittal images of mouse head were obtained using the sequence of Rapid Acquisition with Relaxation Enhancement Three Dimensional (3D) with the following parameters: field of view, FOV = 20 mm × 20 mm, matrix = 512 × 512 (in plane resolution = 39.1 μm × 39.1 μm), slice thickness = 0.2 mm, TR/TE = 800 ms/16.1 ms, number of scan = 16, and acquisition time = 27 min 18 s.

2.4. Ex vivo MRI

2.4.1. Mouse head preparations

The heads of mice were dissected after perfusion fixation. After removal of the marginal skin, the head was immersed in neutralized formaldehyde for 2 days at 4 °C. Subsequently, the head was placed in 4 °C phosphate-buffered saline (PBS) for 2–4 days. Finally, the head was soaked in 5 mM Gd contrast agent (Gadoxetate Sodium, Bayer Yakuhin, Ltd., Tokyo, Japan) for 4–14 days at 22–24 °C before MRI.

2.4.2. MRI

T_1 weighted mouse head images were obtained using the sequence of 3D Fast Low Angle Shot with the following parameters: volume = 15 mm × x 15 mm × 12.6 mm, matrix = 512 × 512 × 252 (resolution = 29.3 μm × 29.3 μm × 50.0 μm), TR/TE = 40 ms/4 ms, number of scan = 8, and acquisition time = 11 h 28 min 7 s. The matrix was zero-field to 1024 × 1024 × 252 using post-processing. The final 3D image resolution was 14.6 μm × 14.6 μm × 50.0 μm.

2.5. Hematoxylin and eosin (HE) stain

After *ex vivo* MRI analysis, the inner ears were fixed using 4 % paraformaldehyde in 0.1 M phosphate buffer and then decalcified for 1 week. Subsequently, samples were dehydrated in an ascending series of ethanol solution and embedded in paraffin (tissue preparation, T580; FALMA, Tokyo, Japan) using Clear Plus (FALMA). Sections with a thickness of 7 μm were prepared using a microtome (RM2145, Leica Microsystems K·K, Tokyo, Japan) and attached to MAS-coated glass slides (Matsunami-glass, Osaka, Japan). Slides were stored at 4 °C until use. After deparaffinization using xylene, hydrophilic treatment was performed using a descending series of ethanol solution. The slides were stained with a hematoxylin solution (FUJIFILM Wako Chemicals Corporation, Osaka, Japan) for 5 min, washed with tap water for 10 min, and subsequently stained using an eosin solution (FUJIFILM Wako Chemicals Corporation) for 3 min. After washing, the slides were dehydrated in an ascending ethanol series, cleared using xylene, and mounted on a cover glass using Entellan (Merck KGaA, Darmstadt, Germany). Slides were observed and analyzed using a Keyence microscope (Keyence Corporation, Osaka, Japan).

3. Results

3.1. In vivo contrast-enhanced MRI analysis

First, MRI analysis of the inner ear was performed in healthy mice administered with a contrast agent. The outline of the cochlear labyrinth and its entire circumference were determined from the acquired MRI images (Fig. 1a). By contrasting the scala vestibuli and scala tympani, the boundary between the scala media was clearly delineated. In addition, the boundaries between the scala media, bone spiral plate, and cochlear axis were visible. However, the boundaries of the other structures were unclear. For *in vivo* MRI analysis, it was possible to determine the areas of endolymph and perilymph; however, it was difficult to obtain information that requires higher resolution, such as structural abnormalities.

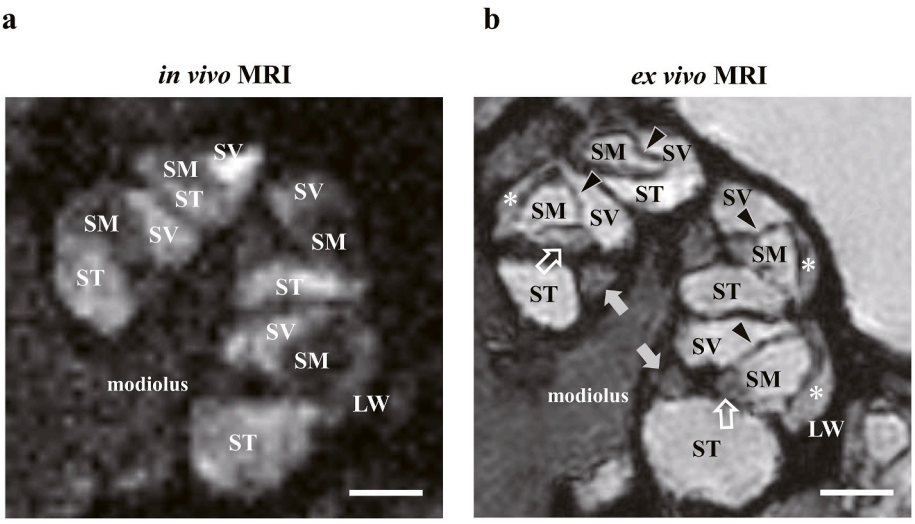

Fig. 1. Representative normal right cochlea images of *in vivo* and *ex vivo* MRI
(a) *in vivo* MRI image. The boundary between the endolymph space and perilymph space was clear and distinguishable. However, the boundaries of other structures were unclear. (b) *Ex vivo* MRI image. The boundary between the scala vestibule and scala media was clearly seen by Reissner's membrane. The structures of the organ of Corti and stria vascularis can now be seen more clearly. SV: scala vestibuli, ST: scala tympani, SM: scala media, and LW: lateral wall. Black arrowheads: Reissner's membrane, white arrows: the organ of Corti, asterisks: stria vascularis and grey arrows: osseous spiral lamina, modiolus. Scale bar: 500 μm.

3.2. Ex vivo contrast-enhanced MRI analysis

Subsequently, we performed *ex vivo* MRI analysis of the excised inner ear. Compared with *in vivo* MRI images, the boundaries of the cochlear structures were more clearly defined in *ex vivo* MRI images. The structure of the organ of Corti in the scala media and the boundary between the endolymph space and stria vascularis were observed (Fig. 1b). Furthermore, we confirmed the boundary between the scala vestibuli and scala media, which are separated by Reissner's membrane. Although *in vivo* MRI analysis did not detect the morphology of

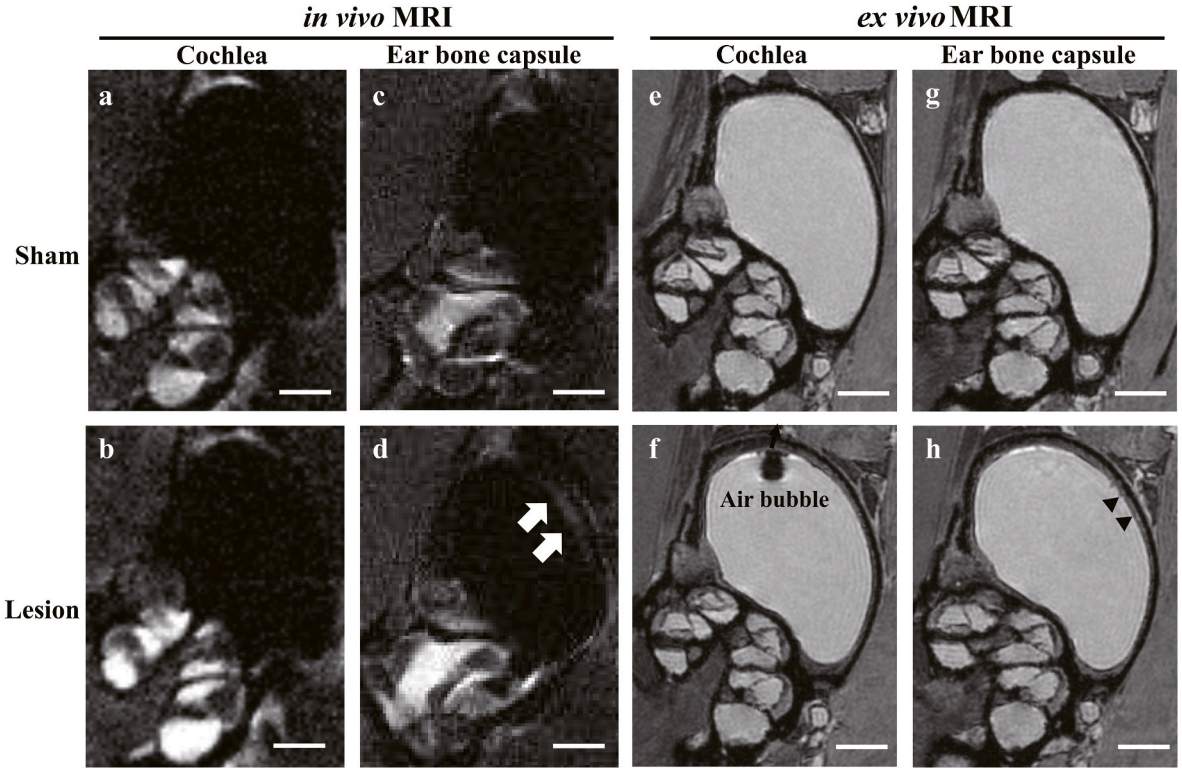

Fig. 2. Representative right cochlea images of *in vivo* and *ex vivo* MRI in LPS-induced otitis media mouse models
(a-d) *in vivo* MRI images. Structural changes in the cochlea were not obvious on the right sham side (a) and left LPS-injected side (b); however, a signal (white arrows) was observed only in the upper part of the ear bone capsule on the left LPS-injected side (d) unlike the right sham side (c). (e–h) *Ex vivo* MRI images. No obvious structural changes were observed in the cochlea on the right sham side (e) and left LPS-injected side (f). However, the mucosa of the left ear bone capsule, which was in direct contact with LPS, was clearly thickened (h: black arrowheads) compared to the sham side (g). Sham: right sham inner ear, LPS: left lipopolysaccharide-injected inner ear. Scale bar: 500 μm.

Reissner's membrane, *ex vivo* MRI analysis revealed that Reissner's membrane had a single thick linear structure (Fig. 1). *Ex vivo* MRI analysis techniques have significantly improved resolution, making it possible to observe the inner ear at higher magnification. Contrast agent infiltration into the endolymph space helped in distinguishing the structures within the endolymph, such as Reissner's membrane and stria vascularis. These findings demonstrate that *ex vivo* MRI analysis is a useful method for the detailed analysis of mouse inner ear structures including Reissner's membrane.

3.3. MRI analysis in LPS-induced otitis media mouse models

Further, we investigated whether our MRI analysis could capture pathological changes in the mouse inner ear using otitis media mouse models. *In vivo* MRI analysis revealed that the contrast agent-induced signal was enhanced in the left cochlear perilymph treated using LPS compared with that in the untreated right cochlear perilymph. However, there was no difference in the volume ratio of cochlear perilymph to endolymph or in their respective structures in the right (sham side) and left (LPS side) inner ears (Fig. 2a and b). In addition, thickening of the mucosal structures was observed in the left ear bone capsule (Fig. 2d), whereas no such thickening was observed in the right ear bone capsule (Fig. 2c). Subsequently, to analyze structural alternation caused by inflammation in detail, *ex vivo* MRI analysis was performed. No differences were observed in the structure of the cochlea between the right and left sides (Fig. 2e and f); however, thickening of the mucous membrane was clearly observed in the left ear capsule (Fig. 2g and h). No structural abnormality was observed in the right ear capsule. No extension of Reissner's membrane due to otitis media was observed (Fig. 2e–h). In summary, by combining the two MRI analysis methods, *in vivo* and *ex vivo*, we were able to capture the inner ear structure and its changes in greater detail.

3.4. Pathological analysis using HE-stained inner ear specimens

Finally, to examine the accuracy of the findings obtained from the MRI analysis, we performed a pathological analysis using HE-stained mouse inner ear specimens. No structural changes were observed in the cochlea, without or with LPS treatment (Fig. 3a and b). In contrast, there was no change in the mucosa of the right ear capsule (Fig. 3c); however, thickening of the mucosa of the left ear capsule was observed (Fig. 3d). Therefore, the pathological analysis using HE-stained specimens revealed similar results as those of the findings from the MRI analysis. Conversely, in HE-stained specimens, the morphology of Reissner's membrane was observed to be loose and extend, which could not reflect the results of *ex vivo* MRI analysis.

In summary, our two types of MRI analyses were found to be superior methods that can be used to understand the structure such as Reissner's membrane and pathology, more accurately.

4. Discussion

In this study, we used 11.7 T upfield MRI for the first time to analyze the structure of the inner ear. Compared with the 9.4 T MRI image of Degerman et al. [4], the entire circumference of the cochlear labyrinth could be clearly distinguished in our MRI image, and the boundaries of the internal and external lymphatic spaces were clearly delineated. Unlike previous MRI analyses, the resolution was clearly improved, and the structure of the inner ear could be clearly observed. However, it was also revealed that even our *in vivo* MRI analysis was insufficient to investigate Reissner's membrane and structural abnormalities in inner ear. In *ex vivo* MRI analysis, the inner ear is directly immersed in the contrast agent; therefore, the boundaries with all structures within the cochlea are clearer than those in the *in vivo* MRI analysis method. Furthermore, the Reissner's membrane could be clearly visualized, albeit with a low signal intensity. In the *ex vivo* MRI analysis method, the inner ear of the mouse is removed immediately after sacrifice; therefore, tissue invasion due to contrast agent immersion is minimal, and it is possible to perform image evaluations that are similar to *in vivo* conditions. In *ex vivo* MRI, the slice thickness is 50 μm, and the planar resolution, including post-processing, is 14.6 μm. Therefore, the Reissner's membrane is almost perpendicular to the slice plane, but since the Reissner's membrane is 10 μm thick, it was possible to observe it. In *ex vivo* MRI analysis, Reissner's membrane was observed as a single linear structure, and for the first time, the exact structure of Reissner's membrane was revealed by MRI analysis.

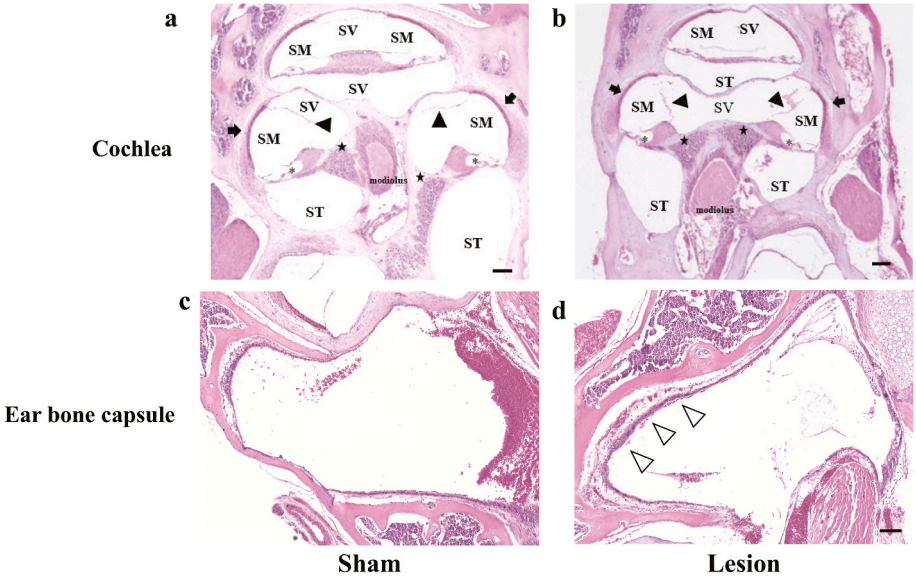

Fig. 3. Representative micrographs of HE-stained cochlea and ear bone capsule in LPS-induced otitis media mouse models
(a-d) No obvious structural changes in the cochlea were noticed between the sham side (a) and LPS-injected side (b), but the mucosa of the left ear bone capsule (white arrowhead), which was in direct contact with the LPS, was clearly thickened in the LPS-injected side (d) compared to the right sham side (c). SV: scala vestibuli, ST: scala tympani, SM: scala media and LW: lateral wall. Black arrowheads: Reissner's membrane, asterisks: the organ of Corti, black arrows: stria vascularis and black stars: osseous spiral lamina, modiolus. Sham: right sham inner ear, LPS: left lipopolysaccharide-injected inner ear. Scale bar: 100 μm.

In the LPS-treated otitis media mouse models, *ex vivo* MRI succeeded in capturing results similar to those of the pathological analysis using HE-stained specimens. Conventionally, the structural analysis of the mouse inner ear is conducted by morphological methods using inner ear sections. However, the fixative and embedding materials used when preparing tissue sections affect the tissue morphology [9], and the structure may be artificially damaged during the analysis process. Such artifacts occur in tissues with numerous cavities, such as the cochlea. Distinguishing endolymphatic hydrops by increasing the endolymph space area is extremely difficult. Reissner's membrane, which is the boundary between the endolymphatic and perilymphatic spaces, is often displaced from its original position during the sectioning and staining processes; therefore, it is difficult to determine whether the expansion of the endolymph space area is a structural change associated with a pathological condition or an artificial change. In fact, the HE staining results did not reflect the *ex vivo* MRI images, and Reissner's membrane was loose and stretched. Judging from the HE staining results alone, we would have mistakenly assumed that endolymphatic hydrops had occurred in the inner ear of the otitis media mouse models (Figs. 2 and 3). There were parts where the Reissner's membrane was cut (Fig. 3a and b); however, it was difficult to determine whether this structural abnormality was artificial. Additionally, it is difficult to capture chronological alterations in the same individual because the inner ear must be removed when preparing tissue sections.

The MRI analysis was developed as a method that can eliminate such artificial flaws in morphological analysis and capture changes over time. Inner ear imaging evaluation using MRI began in 1990 using guinea pigs. Because the analyses were performed using *ex vivo* MRI with the inner ears removed [10,11], it was not possible to perform a longitudinal analysis using living organisms. Since 2010, MRI has been conducted in mice. Although living organisms can be photographed, the resolution of these images was poor. However, the presence or absence of endolymphatic hydrops can be confirmed, and it has been used to evaluate endolymphatic hydrops [12,13]. Thus, improvements in the accuracy of MRI have made it possible to evaluate images even in the small inner ear of mice.

The magnetic field of the MRI we used was 11.7 T, which is the highest magnetic field among existing reports. The inner ear images obtained using our MRI analysis had significantly improved image quality compared with conventional MRI images, similar to the inner ear images obtained by our *in vivo* MRI analysis that had significantly improved image quality compared with existing images; making it easier to understand he endolymph and perilymph spaces and identify areas of structural change. Additionally, biological chronological changes and spatial comprehension improved significantly. However, owing to the difficulty in obtaining clear images such as HE-stained tissue specimens, it has been difficult to perform detailed morphological evaluations of the inner ear using *in vivo* MRI analysis. To overcome these shortcomings, we combined *ex vivo* MRI analysis methods. Using this *ex vivo* MRI analysis, we obtained images with better contrast than those in previous similar analyses. The results of the *ex vivo* MRI analysis reflected those of *in vivo* MRI analysis. Therefore, the first step is to use *in vivo* MRI analysis to examine the timing and individuals in whom major changes such as structural abnormalities occur. At the time points obtained, we recommend removing the inner ear and performing a detailed analysis using clear images obtained by *ex vivo* MRI analysis.

We previously reported the usefulness of analysis methods using 11.7 T MRI. In a study using mouse models with brain injury, *in vivo* MRI analysis identified the detailed location of the brain injury site, and *ex vivo* MRI analysis (diffusion tensor tractography) revealed the left-right differences (the LPS and the contralateral side) in the degree of white matter damage caused by brain contusion [14]. Additionally, we visualized the inflammatory state of the large intestine in a mouse model of ulcerative colitis using T2 images, and analyzed the state of new blood vessels caused by inflammation using magnetic resonance angiography (MRA) [15].

In the present study, our method combined *in vivo* and *ex vivo* MRI analyses, to obtain a detailed overview of the structural changes caused by inflammation. MRI analysis is an excellent technology that can capture the three-dimensional structure of various structures, abnormalities, and changes over time. Our analytical method using 11.7 T MRI is revolutionary and allows us to take full advantage of the strengths of MRI analysis. Especially, precise visualization of the Reissner's membrane in mouse inner ear will enable the analysis of pathological conditions such as endolymphatic hydrops; further, advance the analysis of diseases, such as Meniere's disease that are associated with such pathological conditions. This method is expected to significantly contribute to the research progress in the field of Otolaryngology, including hearing loss.

5. Conclusions

We demonstrated an effective method for imaging analysis of small tissues, such as the mouse inner ear using 11.7 T MRI. Using two methods, *in vivo* and e*x vivo* MRI, for the first time, we succeeded in understanding the fine structure of the mouse inner ear, such as the Reissner's membrane and inflammation state, more accurately. We believe that understanding the exact state of Reissner's membrane *in vivo* will contribute to further progress in the field of otorhinolaryngology.

Funding details

This work was supported by JSPS KAKENHI Grant number JP 23K15862 (Grant-in-Aid for Early-Career Scientists).

Data availability

All relevant data are within the paper and its Supplementary Information files.

CRediT authorship contribution statement

Shotaro Harada: Data curation, Formal analysis, Funding acquisition, Investigation, Visualization, Writing – original draft. **Yoshihisa Koyama:** Conceptualization, Formal analysis, Methodology, Project administration, Validation, Visualization, Writing – original draft, Writing – review & editing. **Yoshichika Yoshioka:** Data curation, Formal analysis, Methodology, Visualization, Writing – review & editing. **Hidenori Inohara:** Supervision, Writing – review & editing. **Shoichi Shimada:** Supervision, Writing – review & editing.

Declaration of competing interest

The authors report no conflict of interest.

Acknowledgement

This research was supported by JSPS KAKENHI Grant number JP 23K15862 (Grant-in-Aid for Early-Career Scientists). We would like to thank Editage (www.editage.com) for English language editing and the Center for Medical Research and Education, Graduate School for Medicine, Osaka University for technical support.

Appendix A. Supplementary data

Supplementary data to this article can be found online at https://doi.org/10.1016/j.bbrc.2024.150153.

References

[1] C.M. Sloan-Heggen, A.O. Bierer, A.E. Shearer, D.L. Kolbe, C.J. Nishimura, K. L. Frees, S.S. Ephraim, S.B. Shibata, K.T. Booth, C.A. Campbell, P.T. Ranum, A. E. Weaver, E.A. Black-Ziegelbein, D. Wang, H. Azaiez, R.J.H. Smith, Comprehensive genetic testing in the clinical evaluation of 1119 patients with hearing loss, Hum. Genet. 135 (2016) 441–450, https://doi.org/10.1007/s00439-016-1648-8.

[2] H. Azaiez, K.T. Booth, S.S. Ephraim, B. Crone, E.A. Black-Ziegelbein, R.J. Marini, A. E. Shearer, C.M. Sloan-Heggen, D. Kolbe, T. Casavant, M.J. Schnieders, C. Nishimura, T. Braun, R.J.H. Smith, Genomic landscape and mutational signatures of deafness-associated genes, Am. J. Hum. Genet. 103 (2018) 484–497, https://doi.org/10.1016/j.ajhg.2018.08.006.

[3] Q. Li, C. Cui, R. Liao, X. Yin, D. Wang, Y. Cheng, B. Huang, L. Wang, M. Yan, J. Zhou, J. Zhao, W. Tang, Y. Wang, X. Wang, J. Lv, J. Li, H. Li, Y. Shu, The pathogenesis of common Gjb2 mutations associated with human hereditary deafness in mice, Cell. Mol. Life Sci. 80 (2023) 148, https://doi.org/10.1007/s00018-023-04794-9.

[4] E. Degerman, R. In 't Zandt, A.K. Pålbrink, M. Magnusson, Vasopressin induces endolymphatic hydrops in mouse inner ear, as evaluated with repeated 9.4 T MRI, Hear. Res. 330 (2015) 119–124, https://doi.org/10.1016/j.heares.2015.05.008.

[5] H.X. Yin, P. Zhang, Z. Wang, Y.F. Liu, Y. Liu, T.Q. Xiao, Z.H. Yang, J.F. Xian, P. F. Zhao, J. Li, H. Lv, H.Y. Ding, X.H. Liu, J.M. Zhu, Z.C. Wang, Investigation of inner ear anatomy in mouse using X-ray phase contrast tomography, Microsc. Res. Tech. 82 (2019) 953–960, https://doi.org/10.1002/jemt.23121.

[6] M. Yamazaki, K.X. Kim, D.C. Marcus, Sodium selectivity of Reissner's membrane epithelial cells, BMC Physiol. 11 (2011) 4, https://doi.org/10.1186/1472-6793-11-4.

[7] T.H. Yoon, M.M. Paparella, P.A. Schachern, C.T. Le, Cellular changes in Reissner's membrane in endolymphatic hydrops, Ann. Otol. Rhinol. Laryngol. 100 (1991) 288–293, https://doi.org/10.1177/000348949110000405.

[8] S.A. Counter, B. Bjelke, T. Klason, Z. Chen, E. Borg, Magnetic resonance imaging of the cochlea, spiral ganglia and eighth nerve of the Guinea pig, Neuroreport 10 (1999) 473–479, https://doi.org/10.1097/00001756-199902250-00006.

[9] J.T. O'Malley, S.N. Merchant, B.J. Burgess, D.D. Jones, J.C. Adams, Effects of fixative and embedding medium on morphology and immunostaining of the cochlea, Audiol. Neurootol. 14 (2009) 78–87, https://doi.org/10.1159/000158536.

[10] A.N. Salt, M.M. Henson, S.L. Gewalt, A.W. Keating, J.E. DeMott, O.W. Henson Jr., Detection and quantification of endolymphatic hydrops in the Guinea pig cochlea by magnetic resonance microscopy, Hear. Res. 88 (1995) 79–86, https://doi.org/10.1016/0378-5955(95)00103-b.

[11] I. Koizuka, Y. Seo, M. Murakami, R. Seo, I. Kato, Micro-magnetic resonance imaging of the inner ear in the Guinea pig, NMR Biomed. 10 (1997) 31–34, https://doi.org/10.1002/(sici)1099-1492(199701)10:1<31::aid-nbm446>3.0.co;2-u.

[12] E. Degerman, R. In 't Zandt, A. Pålbrink, L. Eliasson, P. Cayé-Thomasen, M. Magnusson, Inhibition of phosphodiesterase 3, 4, and 5 induces endolymphatic hydrops in mouse inner ear, as evaluated with repeated 9.4T MRI, Acta Otolaryngol. 137 (2017) 8–15, https://doi.org/10.1080/00016489.2016.1211320.

[13] E. Degerman, R. In 't Zandt, A. Pålbrink, M. Magnusson, Endolymphatic hydrops induced by different mechanisms responds differentially to spironolactone: a rationale for understanding the diversity of treatment responses in hydropic inner ear disease, Acta Otolaryngol. 139 (2019) 685–691, https://doi.org/10.1080/00016489.2019.1616819.

[14] S. Hosomi, T. Watabe, Y. Mori, Y. Koyama, S. Adachi, N. Hoshi, M. Ohnishi, H. Ogura, Y. Yoshioka, J. Hatazawa, T. Yamashita, T. Shimazu, Inflammatory projections after focal brain injury trigger neuronal network disruption: an (18)F-DPA714 PET study in mice, Neuroimage Clin 20 (2018) 946–954, https://doi.org/10.1016/j.nicl.2018.09.031.

[15] Y. Koyama, Y. Kobayashi, I. Hirota, Y. Sun, I. Ohtsu, H. Imai, Y. Yoshioka, H. Yanagawa, T. Sumi, H. Kobayashi, S. Shimada, Author Correction: a new therapy against ulcerative colitis via the intestine and brain using the Si-based agent, Sci. Rep. 12 (2022) 15150, https://doi.org/10.1038/s41598-022-19609-3.